Facile Heterogenization of a Cobalt Catalyst via Graphene Adsorption: Robust and Versatile Dihydrogen Production Systems

Shawn C. Eady, Sabrina L. Peczonczyk, Stephen Maldonado, and Nicolai Lehnert*

Department of Chemistry, University of Michigan,930 North University Ave, Ann Arbor MI 48109
Email: lehnertn@umich.edu

Supporting Information

Table of Contents.

1. Experimental Section.

General Methods.

Chemicals were of highest purity grade commercially available and used without further purification (unless mentioned). Methanol (anhydrous, ACS grade) was purchased from Fisher and distilled over calcium hydride, then degassed via extended nitrogen purges prior to use. Acetonitrile (ACS grade), sodium methoxide, trifluoroacetic acid, hydrochloric acid, potassium ferricyanide, and potassium ferrocyanide were purchased from Fisher. 3,6-dichloro-1,2-benzenedithiol was purchased from Sigma. Graphite powder was purchased from MTI Corp.

Synthesis.

The preparation of the cobalt compound was performed by a method analogous to that reported by McNamara and coworkers:[1]

Tetrabutylammonium Co bis(3,6-dichlorophenyldithiolate) (1). In an inert atmosphere box under N_2 pressure (Inovative Technologies), a solution of 3,6-dichloro-1,2-benzenedithiol (Cl_2bdt) (0.436 g, 2.05 mmol) and sodium methoxide (0.116 g, 2.10 mmol) was added dropwise to a suspension of cobalt(II) sulfate hexahydrate (0.281 g, 1 mmol) in 30 mL of dry methanol. The addition instigated a change in color to deep blue, and the resulting solution was stirred for 2 hours. A solution of tetrabutylammonium bromide (0.340 g, 1.05 mmol) in 5 mL methanol was added at this time, and the solution was stirred for an additional 2 hours. The solvent volume was reduced by vacuum to <10 mL, giving a dark blue precipitate which was filtered and dried. Recrystallization of the solid from dichloromethane/ether yielded (TBA)[$Co(S_2C_6H_2Cl_2)_2$] as a dark blue crystalline solid in 64% yield (0.462 g). Spectroscopic data of the product (see Figure S2) match those available in the literature.[1]

Graphene oxide. Graphene oxide for graphene depositions was prepared via Hummer's method:[2]
sodium nitrate (0.5 g) was added to 23 mL of sulfuric acid in a large beaker and stirred until dissolved. Next, 1 g of graphite powder was added and stirred. After cooling in an ice bath, potassium permanganate (3 g) was slowly added to the suspension, instigating gas formation. The ice-bath was then removed and the temperature of the suspension was brought up to room temperature. The reaction beaker was then placed in an oil bath at 40°C and stirred for 1 hour. The reaction was quenched with the slow addition of 40 mL DI water, causing a gas production of brown vapors. After gas production ceased, the suspension was then further diluted with 40 mL of 10% H_2O_2 solution to convert remaining manganese oxides to inert sulfates, causing a change of the solution to a brown color. The solids were centrifuged and washed extensively with a mixture of 5% H_2SO_4 and 5% H_2O_2. The remaining powders were then washed with DI water until neutral pH was reached. The resulting graphene oxide powder was dried in a vacuum oven at 40 °C to give 1.76 g of graphene oxide.

2. X-ray Photoelectron Spectroscopy (XPS, Maldonado laboratory).

All X-ray photoelectron spectra were acquired with a PHI 5400 analyzer using an Al Kα (1486.6 eV) source without a monochromator. Spectra were recorded without charge neutralization at a base pressure of <2.5 x 10^{-9} Torr. A 6 mA emission current and 10 kV anode HT were used. Survey scans were acquired at a pass energy of 117.40 eV. High-resolution XP spectra of Sn 3d, C 1s, Co 2p and S 2p were recorded at a pass energy of 23.5 eV. The binding energies of all spectra were corrected by using the difference between the observed C 1s peak energy and the peak energy of adventitious carbon (284.6 eV).[3] Spectra were fit with a Shirley type background using CASAXPS version 2.313 software. C 1s spectra were fit with a singlet using 45% Gaussian and 65% Lorentzian line shapes. The full width at half maximum (fwhm) was constrained between 0.6 and 2.0. Additional peaks using the same fitting parameters were used to fit the C-O and C-S signals.

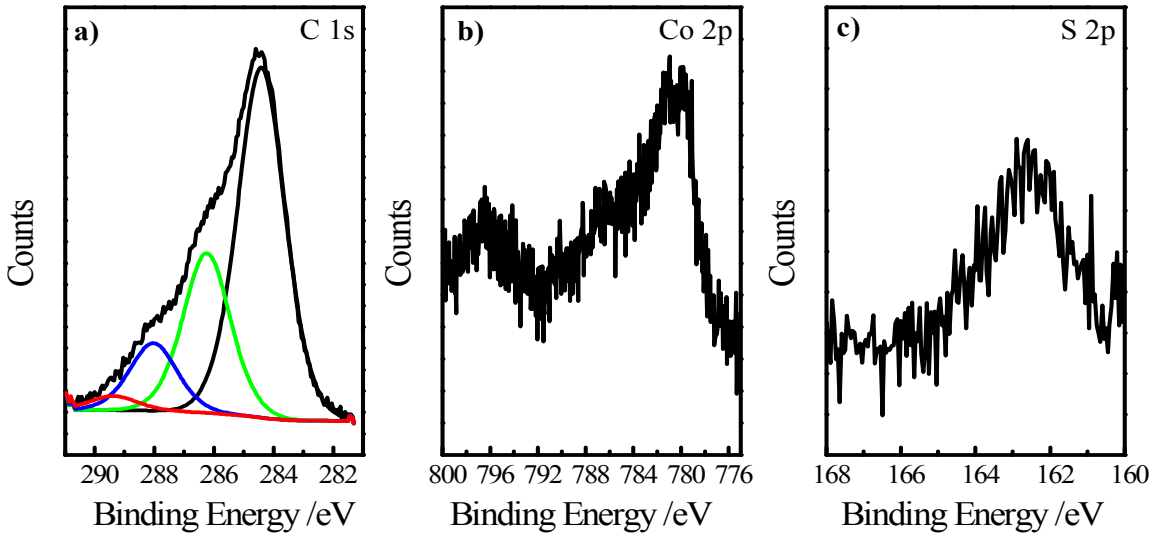

Figure S1. High-resolution (a) C 1s, (b) Co 2p and (c) S 2p XPS data of (TBA)[Co($S_2C_6H_2Cl_2$)$_2$] (**1**) adsorbed on a FTO/graphene electrode **after** electrochemical (CV) TFA titration.

3. UV-Visible Spectroscopy

Electronic absorption spectra were collected at room temperature using an Analytic Jena Specord-600 spectrometer with a WinASPECT (V2.2) interface.

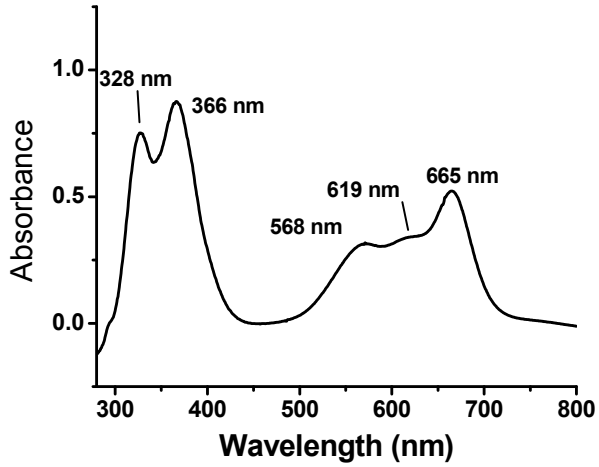

Figure S2. UV-Visible spectrum of (TBA)[Co($S_2C_6H_2Cl_2$)$_2$] (**1**) in acetonitrile solution.

4. Graphene Depositions

0.5 g of graphene oxide (prepared as described above) was added to 30 mL of a 0.1 M sodium carbonate/bicarbonate buffered solution (pH= 9.2) in Millipore water. The solution was stirred extensively for a long time to allow for better graphene oxide sheet separation, becoming more viscous over time. Before deposition, fluorine-doped tin oxide (FTO) coated glass was cleaned by sonication in acetone, ethanol and water. The graphene oxide solution was degassed by a purge with argon gas prior to deposition. For all depositions, the cleaned FTO-glass piece was used as the working electrode in the graphene oxide solution, with a platinum auxiliary electrode and Ag/AgCl reference electrode. In a typical deposition, a CV would be initiated at the open circuit potential (~0 V) and scanned cathodically to -1.4 V, with two cathodic scans for all graphene surfaces used for analysis here. After deposition the surfaces were extensively rinsed with deionized water and sonicated to remove any loose graphene (oxide) from the surface.

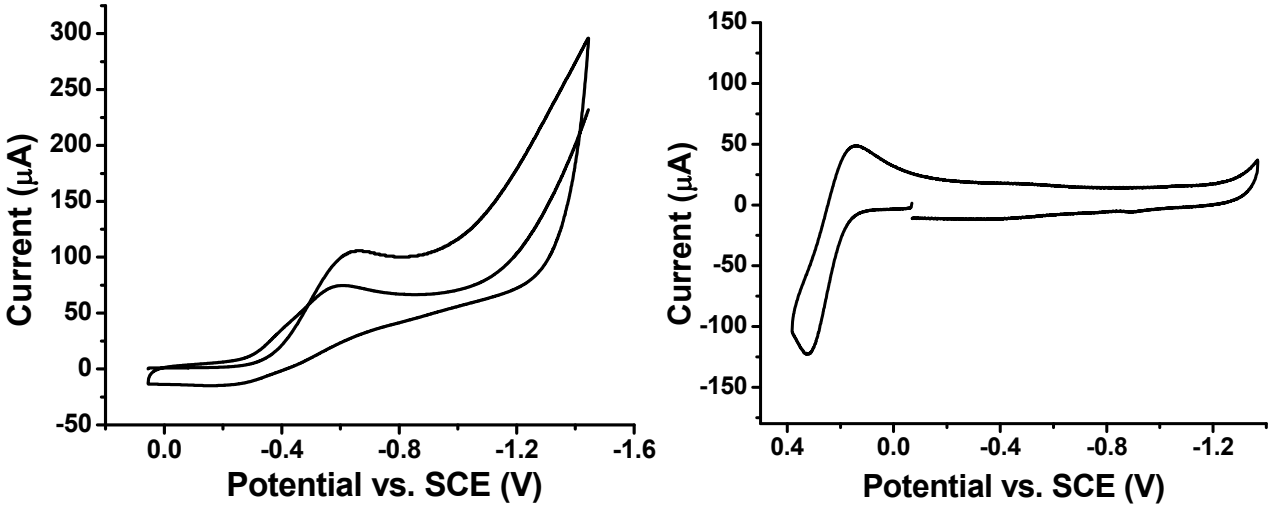

Figure S3. *Left:* Cyclic voltammogram showing graphene deposition on the FTO working electrode surface performed in a 0.1 M sodium carbonate/bicarbonate aqueous buffered solution (pH= 9.2) as described above. Platinum was used as a counter electrode with a Ag/AgCl reference electrode. The scan rate was 100 mV/s. Potentials reported are versus the saturated calomel electrode (SCE). *Right:* Electrochemical window of graphene-coated FTO in aqueous 0.1 M potassium hexafluorophosphate with potassium ferricyanide/ferrocyanide (0.5 mM total) as the internal reference.

5. Catalyst-Adsorbed Electrode Preparation

All catalyst-adsorbed electrode surfaces reported in this work were prepared by soaking the graphene/graphite surface in a 5 mM acetonitrile solution of **1** for 12 hours. After this period, surfaces were extensively rinsed with fresh acetonitrile and subsequently sonicated in a fresh acetonitrile solution for a minimum of 30 minutes to assure any loosely bound catalyst was sufficiently removed prior to electrochemical and XPS analysis.

6. Electrochemical Measurements

All electrochemical measurements were conducted in 18.2 Millipore water. Cyclic voltammetry and controlled potential coulometry were carried out using an Autolab potentiostat with a CHI electrochemical interface. For graphene measurements, the working electrode was a piece of fluorine-doped tin oxide-coated glass (purchased from Pilkington) with thin layers of graphene electrodeposited on the surface by the method described above. For graphite measurements, a highly-ordered edge plane graphite electrode (purchased from Pine instruments) was used. Platinum wire (CH Instrument) was used as the counter electrode in all experiments, and the reference was an

aqueous Ag/AgCl electrode (CH Instruments, saturated AgCl and KCl fill solution). All solutions were prepared with 0.1 M potassium hexafluorophosphate supporting electrolyte as purchased from Fisher and subsequently recrystallized. Argon gas was used to deoxygenate all solutions for a minimum of 30 minutes prior to data collection.

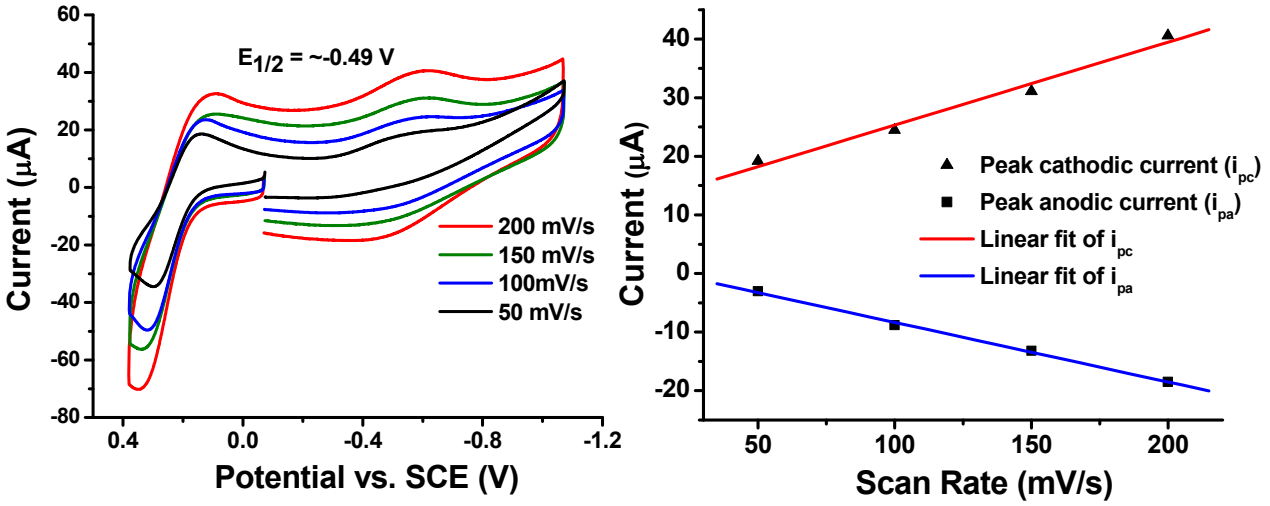

Figure S4. *Left:* Cyclic voltammetry of (TBA)[$Co(S_2C_6H_2Cl_2)_2$] (**1**) adsorbed on a FTO/graphene working electrode at various scan rates. The solution was 0.1 M aqueous potassium hexafluorophosphate, the counter electrode was a platinum wire, and the reference electrode was Ag/AgCl (saturated KCl solution). An equimolar solution of potassium ferricyanide/ferrocyanide (0.5 mM total) was used as an internal reference. Potentials are reported versus the saturated calomel electrode. *Right:* Linear fit of the peak cathodic and anodic current versus the scan rate. The $Co^{III/II}$ couples seen in the FTO/graphene/**1** systems have been observed to vary in potential by as much as 0.03 V. This can be attributed to surface inhomogeneity, possibly caused by a variable number of oxygen containing groups on the graphene surface between different electrodes, and a variation in the number of graphene layers (see next).

Electron transfer kinetics in FTO/graphene/1 and graphite/1 systems

In the FTO/graphene/**1** systems, anodic/cathodic peak separation has been observed to vary with an average separation of 0.18 V. Similarly, the peak separation for an internal standard (potassium ferricyanide) under the same conditions shows a distinct increase from the standard one-electron peak separation of 0.057 V, exhibiting an average ΔE_p of 0.12 V. The cobalt compound consistently maintains a larger separation than the internal standard however, suggesting this separation is in part related to the quasi-reversible nature of the couple in addition to slow diffusion at the FTO/graphene and graphene/catalyst interfaces. In the graphite/**1** system, peak separations are even more substantial for both the internal reference (ΔE_p = 0.25 V) and the cobalt compound (average ΔE_p = 0.35 V), again indicating slow diffusion at the electrode surface in addition to quasi-reversible redox behavior for adsorbed catalysts.

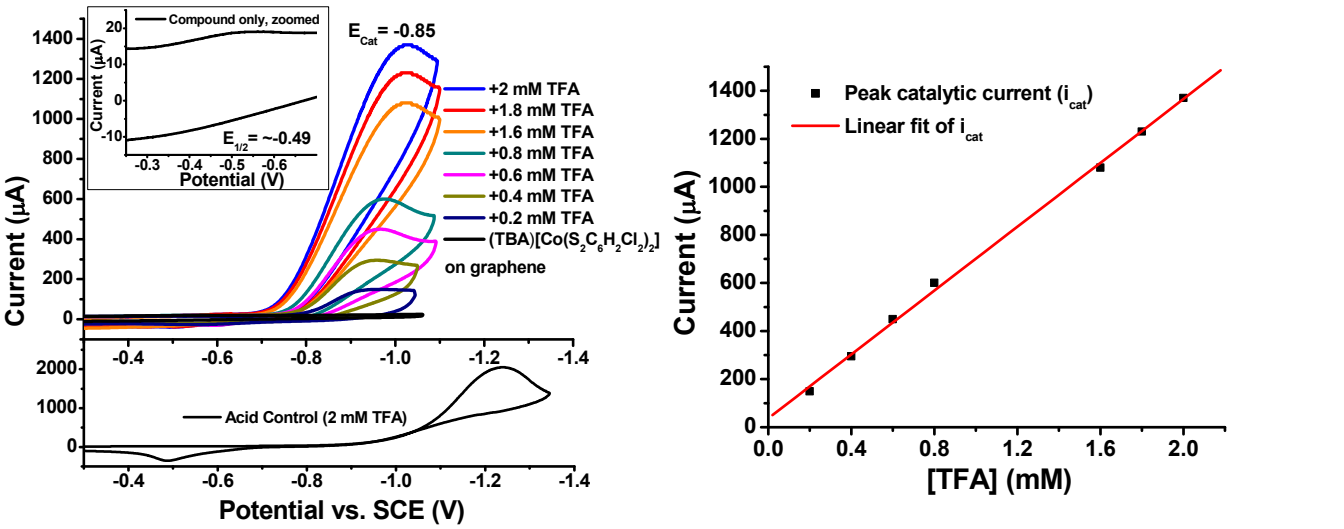

Figure S5. *Left:* Cyclic voltammetry of (TBA)[$Co(S_2C_6H_2Cl_2)_2$] (**1**) adsorbed on a FTO/graphene working electrode with addition of TFA at a scan rate of 100 mV/s. The solution was 0.1 M aqueous potassium hexafluorophosphate, the counter electrode was a platinum wire, and the reference electrode was Ag/AgCl (saturated KCl solution). An equimolar solution of potassium ferricyanide/ferrocyanide (0.5 mM total) was used as an internal reference. Potentials are reported versus the saturated calomel electrode. *Right:* Linear fit of the peak catalytic current versus increasing TFA concentrations, indicating an acid-diffusion controlled process under these conditions.

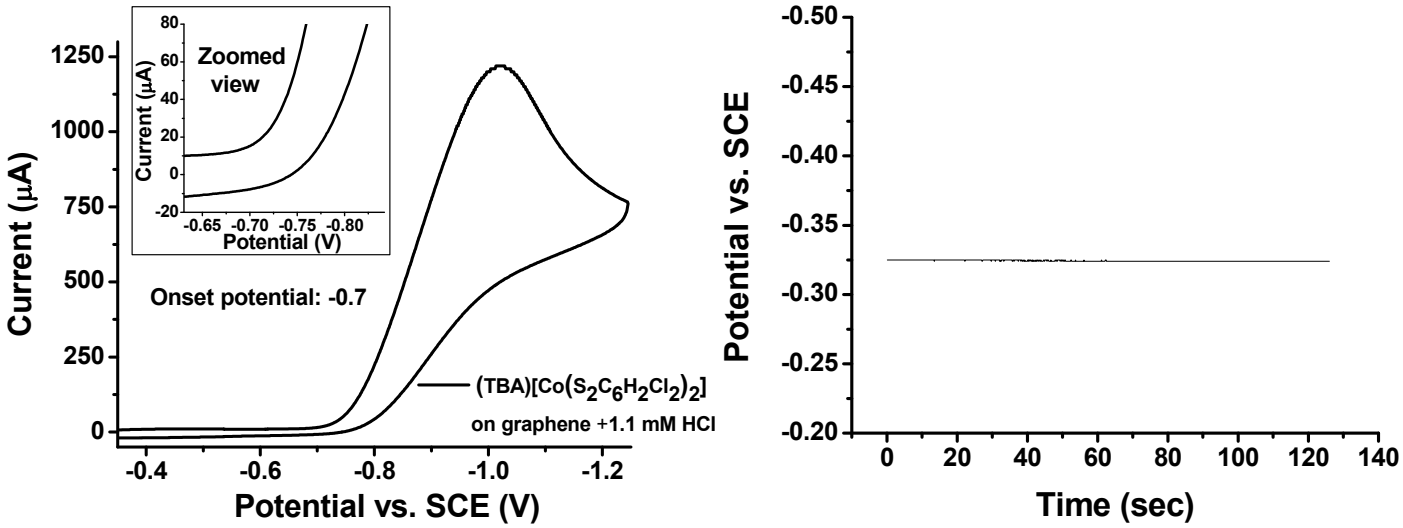

Figure S6. *Left:* Cyclic voltammetry of (TBA)[$Co(S_2C_6H_2Cl_2)_2$] (**1**) adsorbed on a FTO/graphene working electrode in a 1.1 mM HCl solution with a 100 mV/s scan rate. *Right:* Open circuit potential over time of a platinum mesh working electrode in the same acid solution under 1 atm H_2 atmosphere to indicate overpotential. The solution was 0.1 M aqueous potassium hexafluorophosphate, the counter electrode was a platinum wire, and the reference electrode was Ag/AgCl (saturated KCl solution). An equimolar solution of potassium ferricyanide/ferrocyanide (0.5 mM total) was used as an internal reference. Potentials are reported versus the saturated calomel electrode.

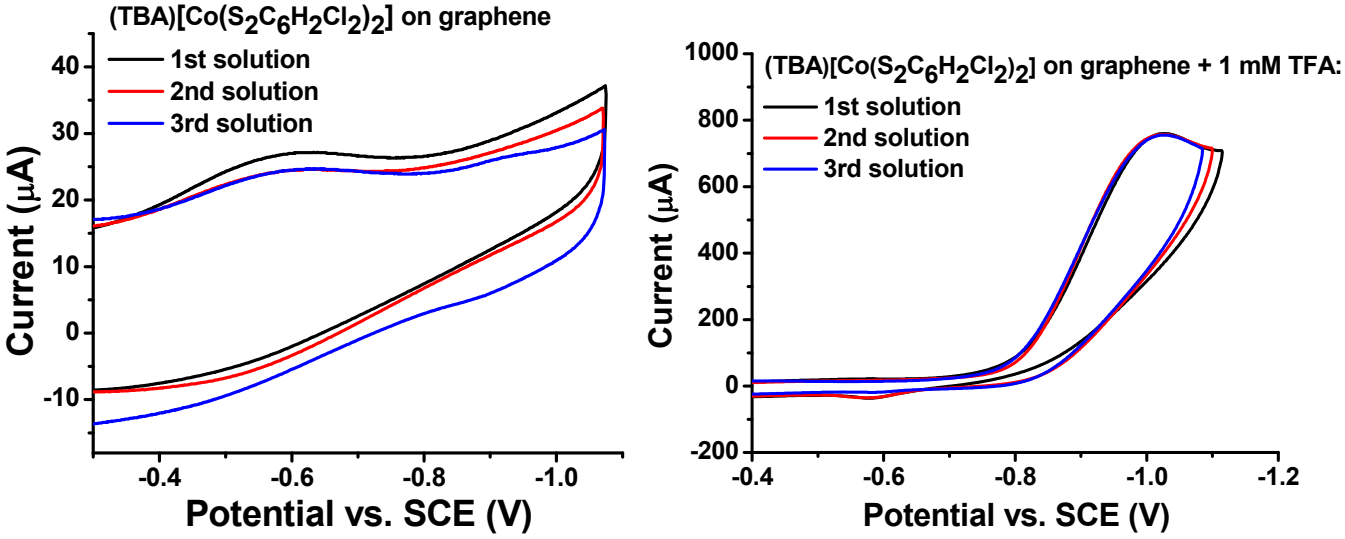

Figure S7. *Left:* overlay of cyclic voltammograms of (TBA)[$Co(S_2C_6H_2Cl_2)_2$] (**1**) adsorbed on a FTO/graphene working electrode in different (consecutively applied) solutions at a scan rate of 100 mV/s. *Right:* Cyclic voltammetry of **1** adsorbed on FTO/graphene with addition of TFA in renewed acidic solutions at a scan rate of 100 mV/s. Each solution was 0.1 M aqueous potassium hexafluorophosphate and 1 mM TFA, with an equimolar solution of potassium ferricyanide/ferrocyanide (0.5 mM total) used as an internal reference. The same electrodes were rinsed and reused for analysis of each solution, with a platinum wire counter electrode and a Ag/AgCl (saturated KCl) reference electrode. The FTO/graphene working electrode was rinsed thoroughly and sonicated briefly in water before analysis in each new solution. Potentials are reported versus the saturated calomel electrode.

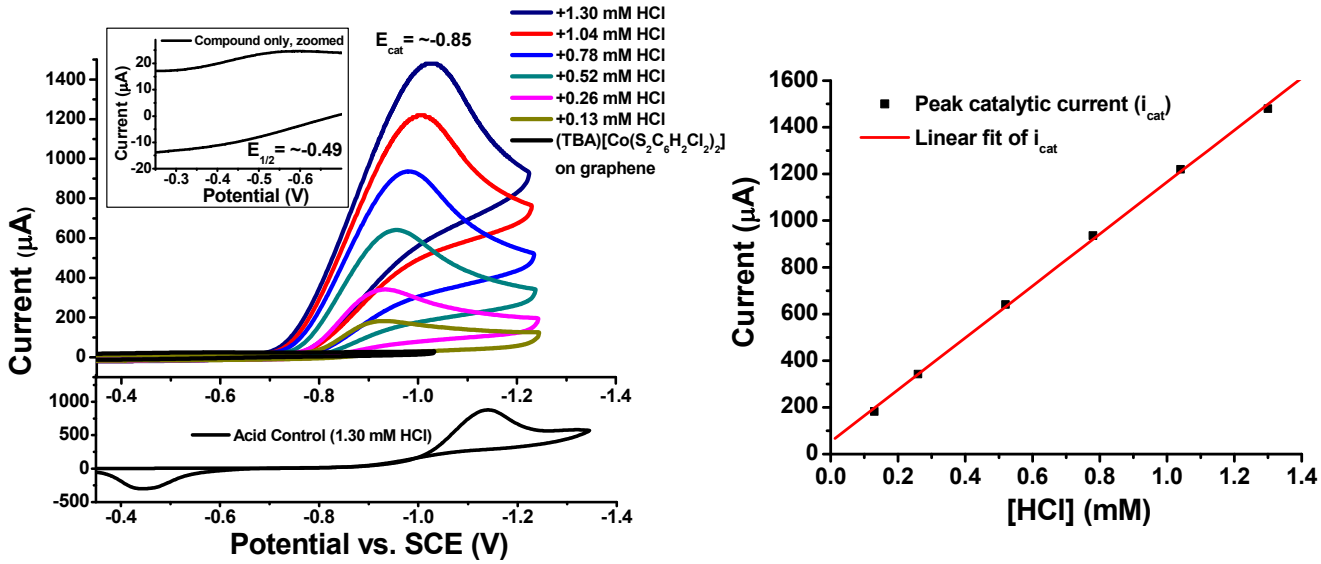

Figure S8. *Left:* Cyclic voltammetry of (TBA)[$Co(S_2C_6H_2Cl_2)_2$] (**1**) adsorbed on a FTO/graphene working electrode with addition of HCl at a scan rate of 100 mV/s. The solution was 0.1 M aqueous potassium hexafluorophosphate, the counter electrode was a platinum wire, and the reference electrode was Ag/AgCl (saturated KCl solution). An equimolar solution of potassium ferricyanide/ferrocyanide (0.5 mM total) was used as an internal reference. Potentials are reported versus the saturated calomel electrode. *Right:* Linear fit of the peak catalytic current versus increasing TFA concentrations, indicating an acid-diffusion controlled process under these conditions.

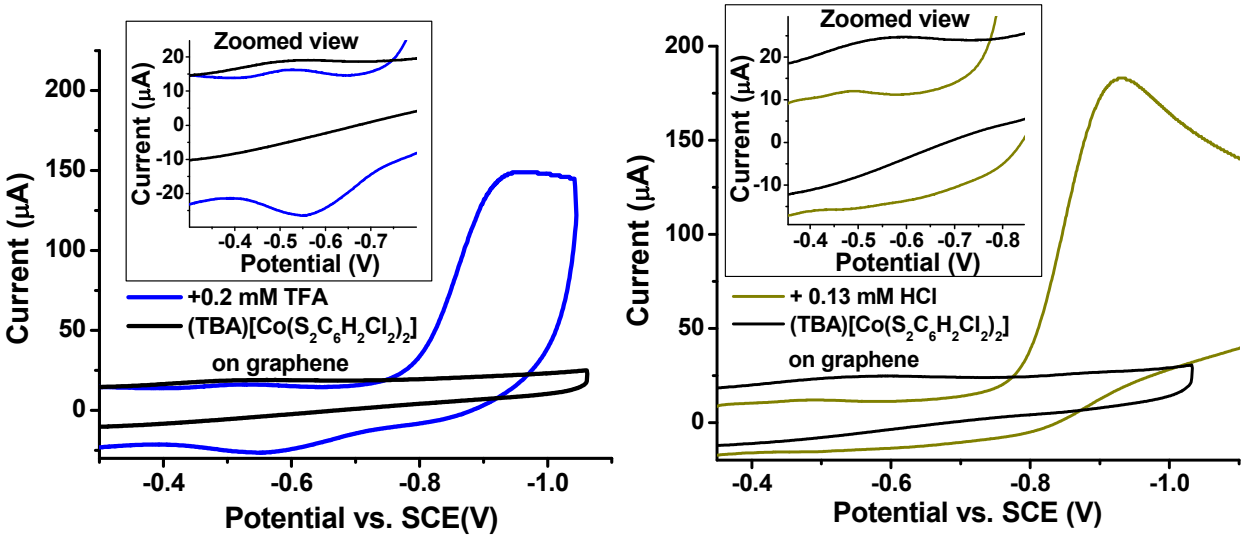

Figure S9. Cyclic voltammetry of (TBA)[$Co(S_2C_6H_2Cl_2)_2$] (**1**) adsorbed on a FTO/graphene working electrode with addition of low concentrations of TFA (*left)* and HCl (*right)*. Both solutions were 0.1 M aqueous potassium hexafluorophosphate, the counter electrode was a platinum wire, and the reference electrode was Ag/AgCl (saturated KCl solution). An equimolar solution of potassium ferricyanide/ferrocyanide (0.5 mM total) was used as an internal reference. Potentials are reported versus the saturated calomel electrode.

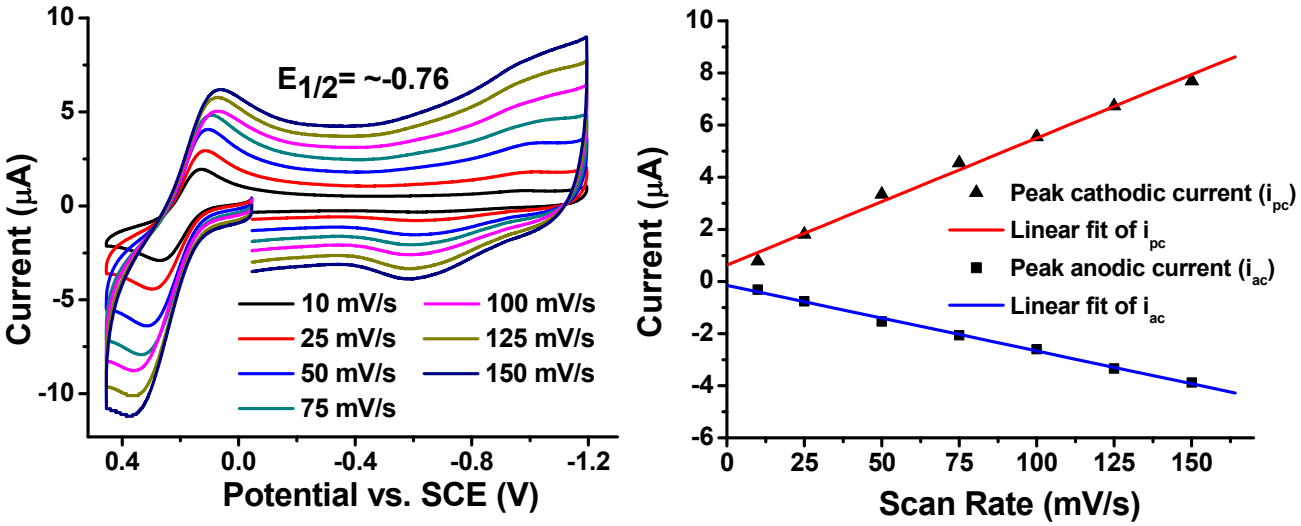

Figure S10. *Left:* Cyclic voltammetry of (TBA)[$Co(S_2C_6H_2Cl_2)_2$] (**1**) adsorbed on a HOPG working electrode at various scan rates. The solution was 0.1 M aqueous potassium hexafluorophosphate, the counter electrode was a platinum wire, and the reference electrode was Ag/AgCl (saturated KCl solution). An equimolar solution of potassium ferricyanide/ferrocyanide (0.5 mM total) was used as an internal reference. Potentials are reported versus the saturated calomel electrode. *Right:* Linear fit of the peak cathodic and anodic currents versus the scan rate.

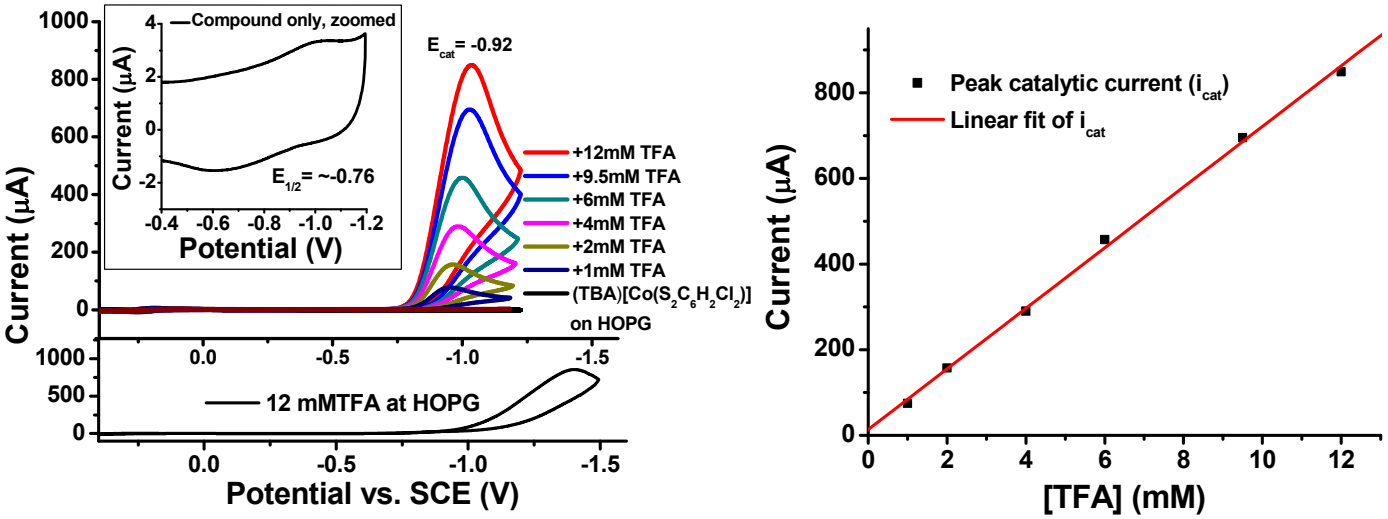

Figure S11. *Left:* Cyclic voltammetry of (TBA)[Co($S_2C_6H_2Cl_2$)$_2$] (**1**) adsorbed on a HOPG working electrode with addition of TFA at a scan rate of 50 mV/s. The solution was 0.1 M aqueous potassium hexafluorophosphate, the counter electrode was a platinum wire, and the reference electrode was Ag/AgCl (saturated KCl solution). An equimolar solution of potassium ferricyanide/ferrocyanide (0.5 mM total) was used as an internal reference. Potentials are reported versus the saturated calomel electrode. *Right:* Linear fit of the peak catalytic current versus increasing TFA concentrations, indicating an acid-diffusion controlled process under these conditions.

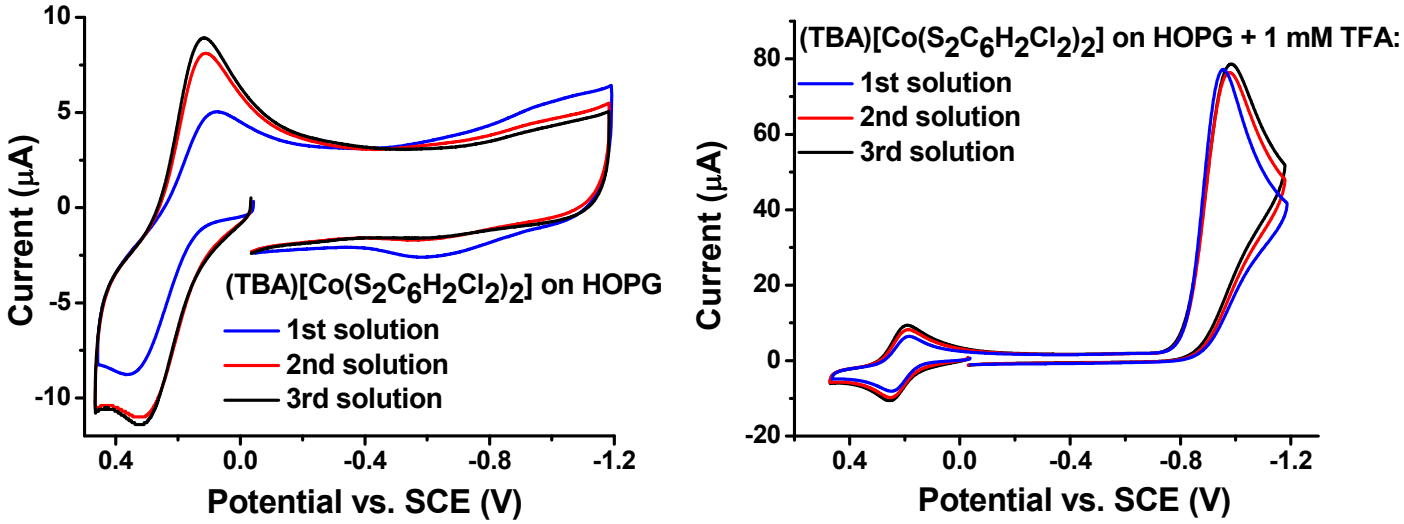

Figure S12. Cyclic voltammetry of (TBA)[Co($S_2C_6H_2Cl_2$)$_2$] (**1**) adsorbed on a HOPG working electrode with addition of TFA in different (consecutively applied) solutions. Each solution was 0.1 M aqueous potassium hexafluorophosphate and 1 mM TFA, with an equimolar solution of potassium ferricyanide/ferrocyanide (0.5 mM total) used as an internal reference. The same electrodes were rinsed and reused for analysis of each solution, with a platinum wire counter electrode and a Ag/AgCl (saturated KCl) reference electrode. The HOPEG working electrode was rinsed thoroughly and sonicated briefly in water before analysis in each new solution. Potentials are reported versus the saturated calomel electrode.

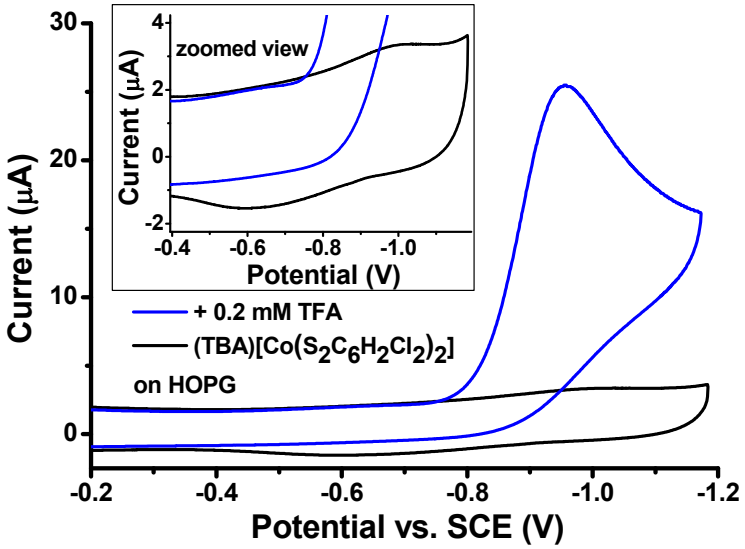

Figure S13. Cyclic voltammetry of (TBA)[$Co(S_2C_6H_2Cl_2)_2$] (**1**) adsorbed on a HOPG working electrode with the addition of a low concentration of TFA. The solution was 0.1 M aqueous potassium hexafluorophosphate, the counter electrode was a platinum wire, and the reference electrode was Ag/AgCl (saturated KCl solution). An equimolar solution of potassium ferricyanide/ferrocyanide (0.5 mM total) was used as an internal reference. Potentials are reported versus the saturated calomel electrode.

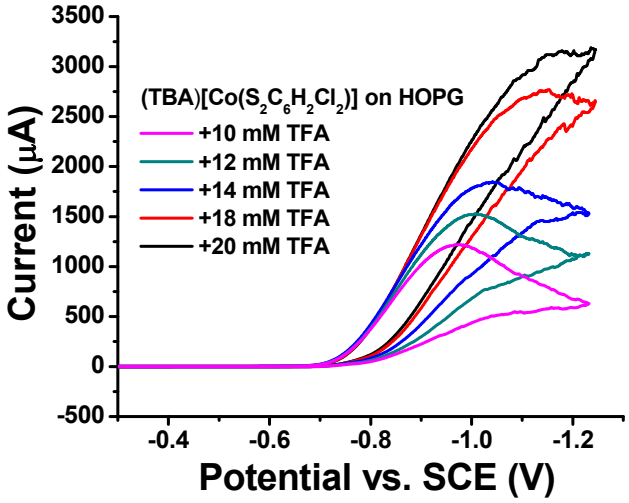

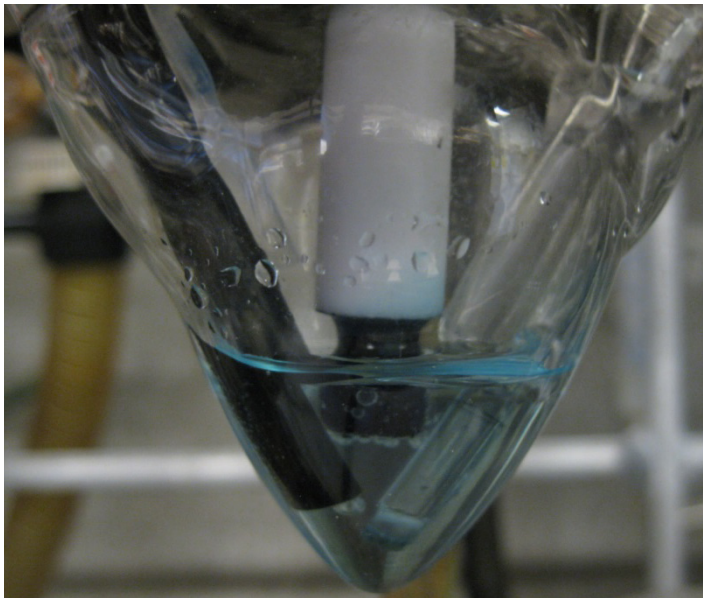

Figure S14. *Left:* Cyclic voltammetry of (TBA)[$Co(S_2C_6H_2Cl_2)_2$] (**1**) adsorbed on a HOPG working electrode in the presence of high concentrations of TFA. The solution was 0.1 M aqueous potassium hexafluorophosphate, the counter electrode was a platinum wire, and the reference electrode was Ag/AgCl (saturated KCl solution). An equimolar solution of potassium ferricyanide/ferrocyanide (0.5 mM total) was used as an internal reference. Potentials are reported versus the saturated calomel electrode. *Right:* Image of the HOPG working electrode (center) generating dihydrogen gas bubbles during the cathodic sweep.

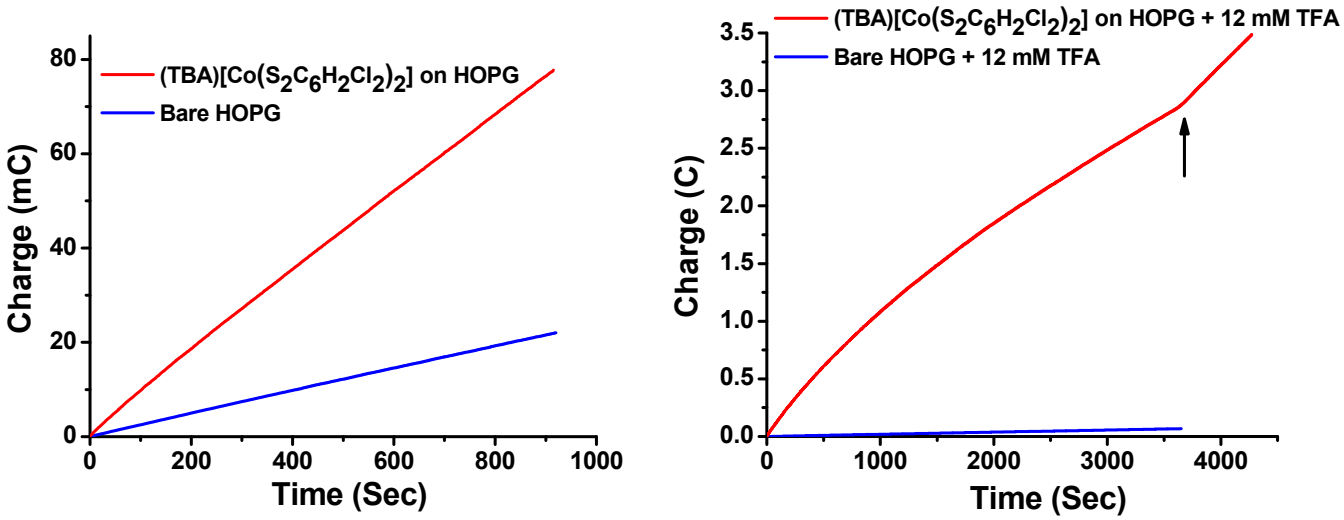

Figure S15. *Left:* Electrolysis of the HOPG working electrode at a potential of -0.95 vs. SCE before and after soaking in a 5mM solution of (TBA)[Co($S_2C_6H_2Cl_2$)$_2$] (**1**) for 12 hours. The quantity of the adsorbed catalyst was not assessed due to a background process occurring in the blank electrolyte solution. *Right:* Electrolysis of the graphite working electrode at a potential of -0.95 vs. SCE in a 12 mM TFA solution before and after soaking in a 5 mM solution of (TBA)[Co($S_2C_6H_2Cl_2$)$_2$] (**1**) for 24 hours. The arrow indicates addition of more TFA. Electrolysis was performed in a two-compartment cell (split into working/reference electrode and counter electrode) with a 0.3 M aqueous potassium hexafluorophosphate solution in both compartments. Potassium ferrocyanide (0.1 M) was added as a sacrificial reductant in the counter electrode chamber. The reference electrode was a Ag/AgCl (saturated KCl) electrode, and a platinum mesh was used as the counter electrode.

7. Gas Chromatography

General Information

Analysis of the product was performed using a SRI 8610C gas chromatograph (GC) equipped with a thermal conductivity detector (TCD) and flame ionization detector (FID), as well as MS13X (6') and Hayesep-D (6') columns using Argon (99.999% pure) as the carrier gas. For the bulk electrolysis experiments, dinitrogen was used as the sample carrier gas at a flow rate of 2.6 mL/min and injections to the detector were made every ten minutes.

Dihydrogen Measurements

Dihydrogen evolution volumes were determined based on the average dihydrogen evolution rates observed at the ten minute intervals. Based on these rates, the H_2 production volumes over each ten minute time span were estimated. Cumulative volumes were obtained by taking the sum of the aforementioned volumes from each time span. Faradaic efficiency was calculated as the molecular sum of evolved dihydrogen divided by half the total charge passed in the same time frame, and was determined to be ~106% based on these methods. The slight excess in efficiency over quantitative yield has been attributed to the difficulty in accurate manual measurement of the flow rates at such low levels, as well as the inherent mathematical error involved with estimation of dihydrogen evolution based on periodic injections.

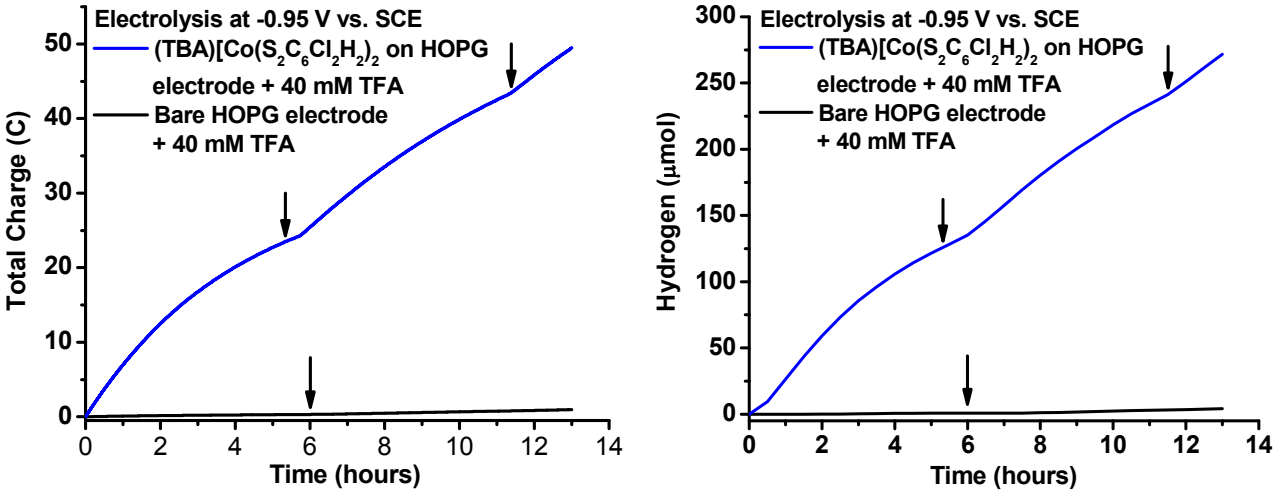

Figure S16. Electrolysis of HOPG electrodes at a potential of -0.95 vs. SCE with 40 mM TFA before and after soaking in a 5mM solution of (TBA)[$Co(S_2C_6H_2Cl_2)_2$] (**1**) for 12 hours. *Left:* Charge accumulation from the electrolysis over time. *Right:* dihydrogen evolution as directly measured by gas chromatography. Arrows on both plots indicate time points at which supplemental TFA was added (equal to initial aliquot). Electrolysis was performed in a two-compartment cell (split into working/reference electrode and counter electrode) with a 0.3 M aqueous potassium hexafluorophosphate solution in both compartments. Potassium ferrocyanide (0.3 M) was added as a sacrificial reductant in the counter electrode chamber. The reference electrode was a Ag/AgCl (saturated KCl) electrode, and a platinum mesh was used as the counter electrode.

8. Determination of Catalytic Turnover Frequencies

The proton reduction activity rates for the FTO/graphene- and graphite-adsorbed catalyst systems were assessed both by methods reported by Bard and Faulkner (**equation 1**)[4] and by the 'foot-of-the-wave' method[5]:

Bard and Faulkner

For both FTO/graphene- and graphite-adsorbed systems acid concentrations used for analysis were below the maximum activity levels (activity saturation), in the FTO/graphene system due to the substantial tin oxide reduction seen at high acid concentrations, and in the graphite system due to disruption of the voltammogram signals by H_2 production at high acid concentrations (**Figure S14**) as well as background acid reduction at graphite under these conditions. Rates predicted by this method are thus expected to be an underestimate of the true TOF under acid saturation.

$$\textbf{(1)}\quad \frac{i_{cat}}{i_p} = \frac{2}{0.446}\sqrt{\frac{RTk_{obs}}{Fv}}$$

Here, i_{cat} and i_p are the peak cathodic current in the presence and absence of acid (respectively), ν is the scan rate [V/s], F is Faraday's constant, and k_{obs} is the observed catalytic rate.

For the FTO/graphene/**1** system, analysis in the presence of trifluoroacetic acid with a concentration of 2 mM gives an i_{cat}/i_p ratio of 72.11, and is predicted by **equation 1** to have a rate of 1,007 s^{-1}. Analysis in the presence of hydrochloric acid with a concentration of 1.3 mM gives an i_{cat}/i_p ratio of 60.16, and is predicted to have a rate of 701 s^{-1}. In the graphite/**1** system, activity with an acid concentration as high as 12 mM TFA can be observed without significant voltammogram distortion, giving an i_{cat}/i_p ratio of 252.68, and is predicted to have a rate of 6,182 s^{-1}.

Activities obtained by this equation for the FTO/graphene/**1** and graphite/**1** systems in subsequent (fresh) acid solutions can be assumed to be very similar to this based on the consistent current responses observed with identical acid concentrations (**Figures S7 & S12**) , thus giving a consistent i_{cat}/i_p ratio and predicted TOF.

Foot-of-the-wave rate analysis

Voltammetry plots of the catalyst-soaked surfaces in the presence of acid were plotted according to methods reported by Saveant and coworkers[5], where E is the observed potential (reported vs. SCE), $E^0(PQ)$ is the potential at the half-wave maximum for the catalytic wave, i is the observed current, and $i^0(p)$ is the peak current of the cathodic wave for the catalyst-soaked surfaces in the absence of acid. Plotting the ratio of $(i/i^0(p))$ following **equation 2** afforded the curves seen on the right in **Figures 16-18,** the base of which was fitted linearly. The slope of this fit provides access to the molar rate constant via **equation 3**.

(2) $$\frac{1}{1+ exp\left[\frac{F}{RT}\left(E-E^0_{PQ}\right)\right]}$$

(3) $$M = 2.24\sqrt{\frac{RT}{Fv}}\sqrt{2kC^0_A}$$

Here, M = slope, $C^0(a)$ is the substrate (acid) concentration [M], and ν is the scan rate [V/s].

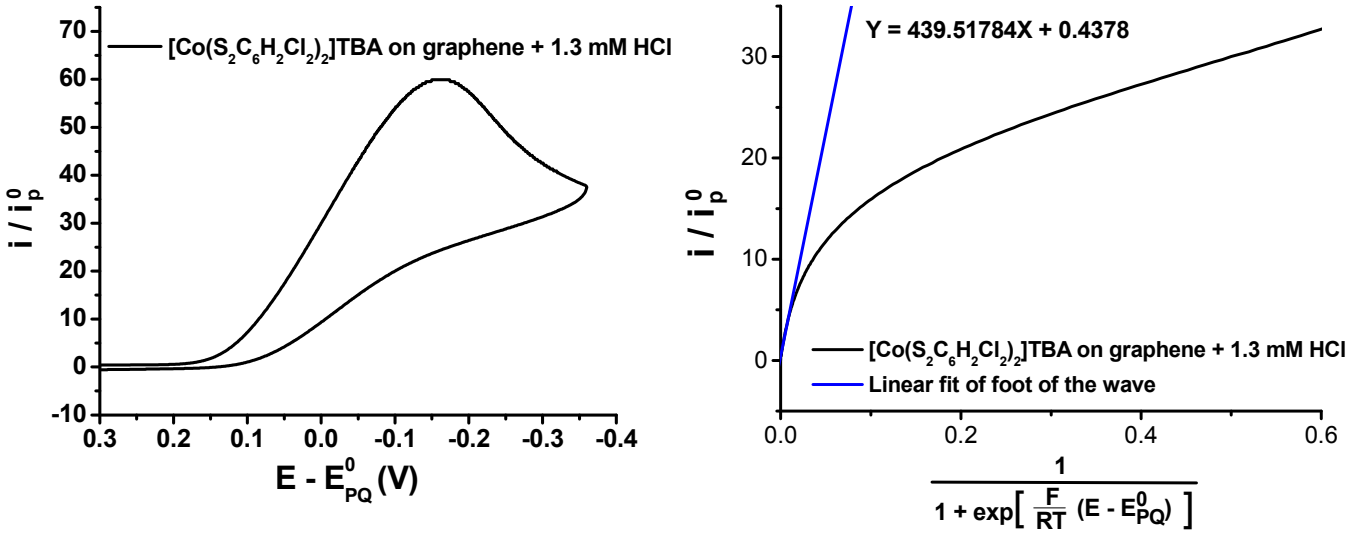

Figure S17. Foot-of-the-wave analysis of (TBA)[$Co(S_2C_6H_2Cl_2)_2$] (**1**) on FTO/graphene in the presence of 1.3 mM HCl.

For **1** adsorbed on FTO/graphene with 1.3 mM HCl, foot-of-the-wave analysis gives a slope of 439.52, resulting in a rate of 5.77 * 10^7 M^{-1} s^{-1} (from **equation 3**).

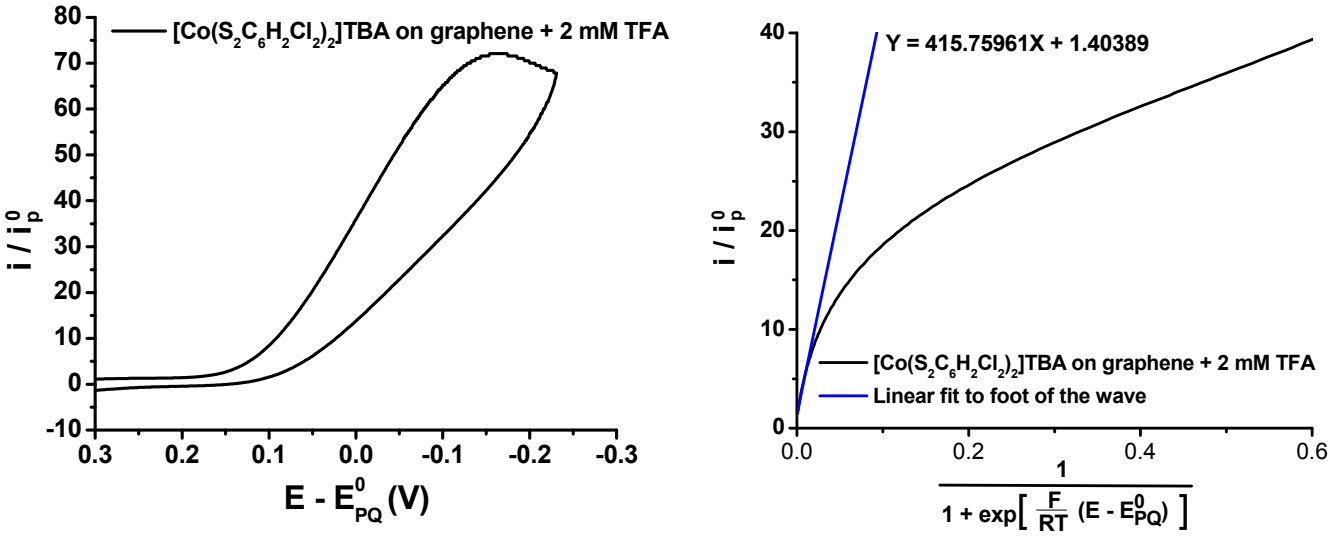

Figure S18. Foot-of-the-wave analysis of (TBA)[$Co(S_2C_6H_2Cl_2)_2$] (**1**) on FTO/graphene in the presence of 2 mM TFA.

For **1** adsorbed on FTO/graphene with 2 mM TFA, foot-of-the-wave analysis gives a slope of 415.76, resulting in a rate of 3.35 * 10^7 M^{-1} s^{-1} (from **equation 3**).

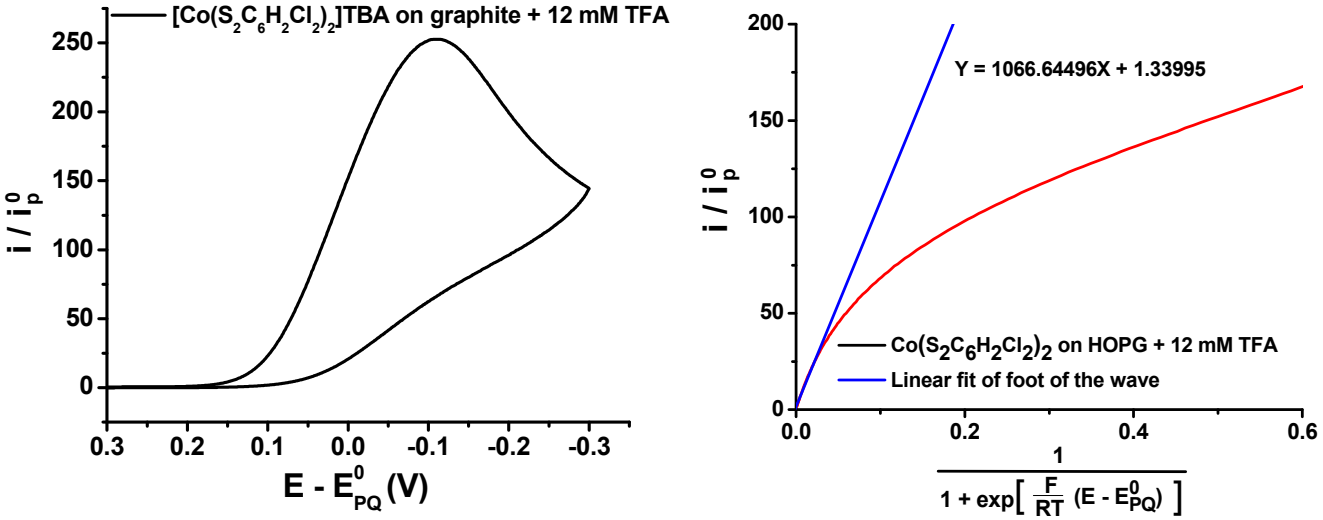

Figure S19. Foot-of-the-wave analysis of (TBA)[$Co(S_2C_6H_2Cl_2)_2$] (**1**) on graphite in the presence of 12 mM TFA.

For **1** adsorbed on graphite with 12 mM TFA, foot-of-the-wave analysis gives a slope of 1066.65, resulting in a rate of 3.68 * 10^7 M^{-1} s^{-1} (from **equation 3**).

REFERENCES

[1] W. R. McNamara, Z. Han, C. J. Yin, W. W. Brennessel, P. L. Holland and R. Eisenberg, *Proc Natl Acad Sci U S A,* 2012, **109**, 15594.
[2] W. S. Hummers and R. E. Offeman, *J. Am. Chem. Soc.,* 1958, **80**, 1339.
[3] J. A. Haber and N. S. Lewis, *J. Phys. Chem. B,* 2002, **106**, 3639.
[4] A. J. Bard and L. R. Faukner, *Electrochemical Methods: Fundamentals and Applications*, **2000**, p.
[5] C. Costentin, S. Drouet, M. Robert and J.-M. Savéant, *J. Am. Chem. Soc.,* 2012, **134**, 11235.